ACS OMEGA

http://pubs.acs.org/journal/acsodf

Article

Fabrication of Transparent Silica/PEG Smooth Thin Coatings on Polymeric Films for Antifogging Applications

Naftali Kanovsky and Shlomo Margel*

Cite This: *ACS Omega* 2022, 7, 20505−20514

Read Online

ACCESS | Metrics & More | Article Recommendations | Supporting Information

ABSTRACT: Fog accumulation on surfaces typically has a negative effect by reducing their transparency and efficiency. Applications such as plastic packaging, agricultural films, and particularly many optical devices suffer from these negative effects. One way to prevent fogging is to coat the substrate with an antifogging coating having a smooth surface and hydrophilic surface chemical groups. This causes the fog water droplets that come into contact with the substrate to completely flatten across its surface, thus retaining transparency. These coatings are mostly relegated to laboratory research due to their insufficient stability and costly synthetic processes. We proposed the use of organically modified silica particles consisting of a mixture of tetraethyl orthosilicate and methacryloxypropyltriethoxysilane, which were grown *in situ* in the presence of a corona-activated polyethylene film, thus providing a thin siloxane coating containing activated double bonds. An additional coating of poly(ethylene glycol) diacrylate was then spread on the coated film and polymerized via UV curing. The *in situ* process and UV curing anchored the coating to the substrate through covalent bonds, which provided additional stability. This coating exhibited low surface roughness and contact angle, which resulted in excellent antifogging properties when exposed to a hot-fog test. Furthermore, the antifogging coating retained its properties after 10 hot-fog cycles, indicating the high coating stability. Additionally, the coating was found durable to immersion in aqueous pH levels 1−13 and detergent solutions as well as to tape test applications and sand test. This coating was compared to a commercially available antifogging spray, which was used to coat a polyethylene film. This resulted in excellent initial antifogging properties, which decreased after exposure to durability tests. The results of the *in situ* coating process indicate its potential uses for industrial applications.

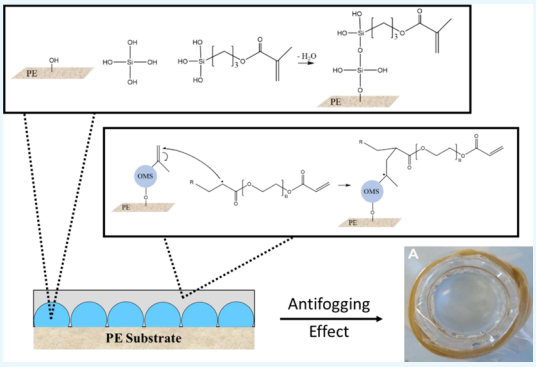

1. INTRODUCTION

Fogging is a phenomenon in which an accumulation of small water droplets condenses on solid surfaces when certain temperature and humidity conditions are met. These small droplets negatively affect the transparency and other optical properties of the fogged surfaces, which is a result of the scattering of light waves caused by the droplets causing a reduction in light transmitted through the surface. Fogging is known to reduce the efficiency and visibility of many devices, which negatively affect applications such as plastic packaging, agricultural films, and many optical devices, such as lenses, mirrors, windshields, and visors.[1−6] Three approaches are typically used to mitigate the accumulation of fogging on specific surfaces: (1) by controlling the surrounding temperature and humidity, thus preventing surface water condensation, (2) superhydrophobic surfaces that repel the droplets from adhering to the surface,[7,8] and (3) superhydrophilic surfaces that flatten the droplets across the surface.[9,10] Superhydrophobic surfaces are less frequently used due to the sophisticated surface design, e.g., hierarchical surface topography, needed to repel the small water droplets. These designs are usually synthetically complicated and have less practical antifogging uses.[11,12] Rough surfaces are needed to achieve superhydrophobicity in part due to hydrophobic air pockets forming between the droplet and rough surface topography.[13] This effect is not achievable with fog formation since the initial fog droplets are too small to form the necessary air pockets. This causes the small droplets to condense on the surface, thus losing the antifogging effect.[3] In addition, rougher surfaces tend to be less transparent, which is an essential property for antifogging surface applications.[14] Superhydrophilic surfaces tend to need simpler surface qualifications, e.g., smooth surface topography, which makes them a more likely candidate for practical antifogging applications.[15,16] As stated previously, surfaces treated with a superhydrophilic layer will cause the droplet to completely flatten on the surface, which will form a continuous thin layer of water. This is due to the strong hydrogen bond interactions between the water droplets

Received: December 26, 2021
Accepted: March 28, 2022
Published: June 6, 2022

ACS Publications

© 2022 The Authors. Published by American Chemical Society

https://doi.org/10.1021/acsomega.1c07293
ACS Omega 2022, 7, 20505−20514

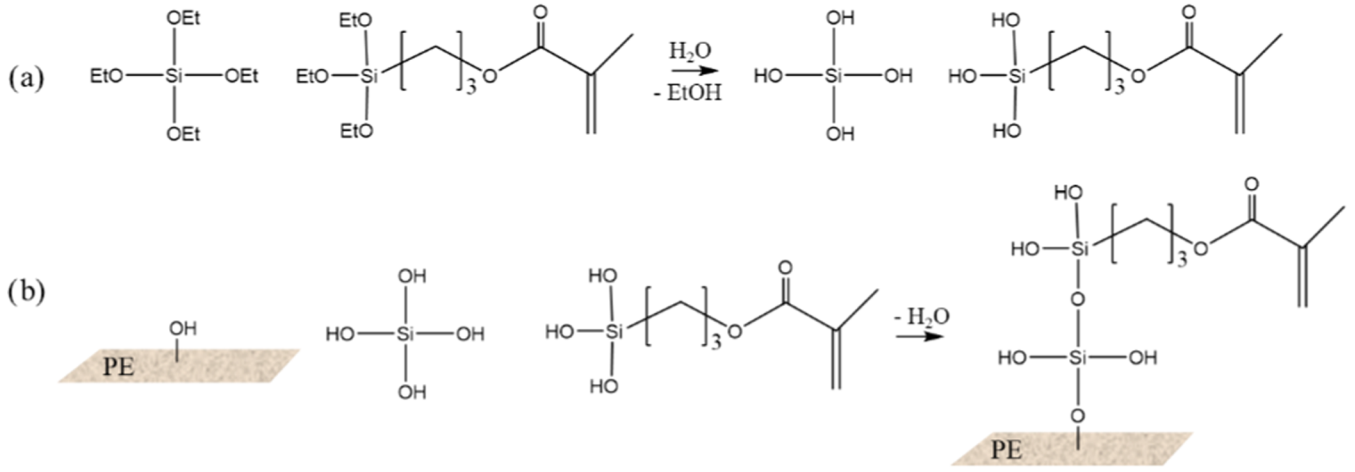

Figure 1. Mechanism for the modified Stöber method, where the ethoxy groups of TEOS and MPTES undergo hydrolysis (a) and then condensation reactions occur between the hydrolyzed silanes as well as with the oxidized PE surface (b).

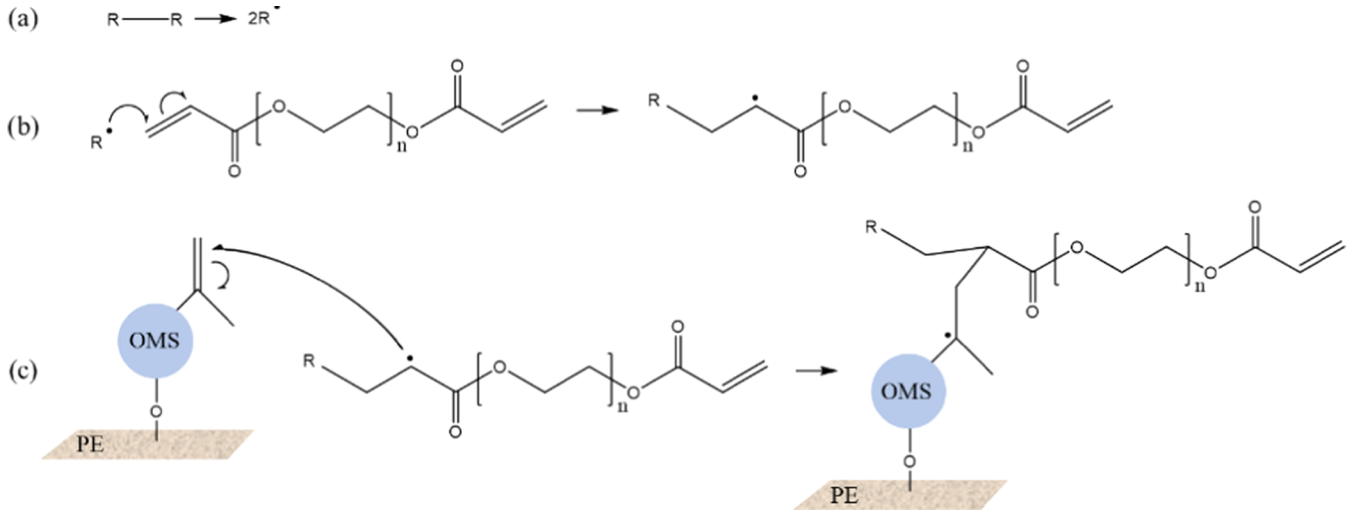

Figure 2. Mechanism for the radical polymerization of PEGDA with the methacrylate groups on the OMS particle. Homolytic cleavage of the photoinitiator into radicals occurs under UV radiation (a) which reacts with the alkene groups of PEGDA (b). The radicalized PEGDA molecule is able to further react with the methacrylate groups on the OMS particle (c).

and the hydrophilic chemical groups present on the surface. This thin water layer significantly reduces the light scattering effects, which retains the transparency of the coated substrate.[16] Hydrophilic surfaces with contact angles below 40° are typically explored for antifogging purposes.[17] These antifogging surfaces are comprised of hydrophilic chemical surface groups, such as hydroxyl, carboxyl, and amine groups, and are typically micrometrically flat, although certain roughened surfaces were also reported to exhibit antifogging properties.[18] Currently, antifogging coatings are mostly relegated to laboratory research due to their insufficient stability in real-world settings, nonenvironmental materials, and costly synthetic processes.[19−21]

Here, we propose a novel method to achieve stable antifogging coatings on polymeric films, e.g., polyethylene (PE) films, using simple synthetic methods. This is done using a modified *in situ* Stöber method,[22] where the monomer tetraethyl orthosilicate (TEOS) and a second organically modified silicate, methacryloxypropyltriethoxysilane (MPTES), are polymerized in the presence of an oxidized polymeric film such as a corona-treated PE film. Polymerization of the silane monomers occurs through hydrolysis of the silane ethoxy groups (Figure 1a). Subsequently, the hydrolyzed silanes react with each other and with the oxidized polymer surface through condensation reactions, which result in the formation of Si−O−Si bonds (Figure 1b). This reaction continues until particles are formed in solution and on the polymer surface.

In this study, the resulting product is an organically modified silica (OMS) particle coating strongly bonded to the surface of the activated PE film. The second coating of poly(ethylene glycol) diacrylate (PEGDA) and photoinitiator was then spread on the coated PE film, which underwent UV curing. The UV light results in a homolytic cleavage of the photoinitiator into radicals (Figure 2a), which initializes the radical polymerization process of PEGDA (Figure 2b). The radicals react with other PEGDA alkene groups and the alkene groups located on the surface of the OMS particles (Figure 2c).

Both corona and UV treatments are needed to anchor all coating components to the film for a stable surface coating. Corona treatment of the film, prior to coating, adds different

https://doi.org/10.1021/acsomega.1c07293
ACS Omega 2022, 7, 20505−20514

oxygen groups to the film surface, which reacts with hydrolyzed silane monomers during the Stöber synthesis to produce covalently bound OMS particles. This was previously reported using a similar *in situ* synthesis on PE using exclusively TEOS as the monomer.[18] In that study, SiO_2 particles were prepared separately after which a corona-treated PE film was placed in the solution for 4 hours. This resulted in an insignificant concentration of surface-bound particles, which indicates that the particles grown *in situ* were covalently bonded and not attached through hydrogen bonds. The OMS particles contain acrylate groups from the MPTES monomer, which participate in the radical polymerization of PEGDA during the second coating step. This anchors the polymerized PEGDA coating to the film surface through the activated double bonds of the OMS particles, which adds stability to the coating.

This coating process has a number of advantages over other reported antifogging processes: (1) The *in situ* process results in strong chemical and self-cross-linked bonds with the substrate, which enhances coating adhesion and durability.[23,24] (2) No primers are necessary to adhere the coating to the surface since all of the coating components are covalently bonded to the surface.[3,24,25] (3) Simple and environmentally friendly chemistry and materials are used to prepare the coating.[20,26,27] (4) Antifogging additives are often prepared separately before coating, which adds further steps to the process including preparation, separation, and drying, which are avoided using this *in situ* process.[19,25,28]

This novel research focuses on the *in situ* synthesis of antifogging coatings using OMS particles combined with polymerized PEGDA chains covalently bonded to a PE film. Furthermore, this research investigated the effects of the photoinitiator at different concentrations using HRSEM, ATR, AFM, contact angle, UV−VIS spectroscopy, and hot-fog tests. Additionally, a commercially available antifog spray (Zeiss antiFOG kit) was used to coat a PE film, which was tested to discern the advantages of the current antifogging coating.

2. EXPERIMENTAL SECTION

2.1. Materials. The following analytical grade chemicals were purchased from Sigma-Aldrich and used without further purification: ethanol absolute anhydrous (EtOH, HPLC), ammonium hydroxide (NH_4OH, 28%), tetraethyl orthosilicate (TEOS, 99%), poly(ethylene glycol) diacrylate 400 (PEGDA), and 2-hydroxy-4′-(2-hydroxyethoxy)-2-methylpropiophenone (Irgacure 2959). Methacryloxypropyltriethoxysilane (MPTES) was purchased from J&K Scientific Ltd. Double distilled water (DDW) was obtained from a TREION purification system. Nontreated and air-corona-treated polyethylene films were provided by Poleg Ltd., Israel.

2.2. Methods. *2.2.1. In Situ Preparation of Organically Modified and Nonmodified SiO_2 Particle Thin Coatings on PE Films.* Colloidal (free) and surface-bound organically modified SiO_2 (OMS) particles were prepared using a modified Stöber polymerization process of TEOS and MPTES in the presence of PE films (5 × 8 cm^2). In a typical experiment, the PE film was first treated with corona (300 W·min/m^2) for 5 seconds and then inserted into a 50 mL Falcon tube, where the synthesis took place. Briefly, 18.75 mL of EtOH, 6.65 mL of DDW, 0.45 mL of NH_4OH (28%), 1.35 mL of TEOS, and 0.15 mL of MPTES were added to the tube. The solution was then shaken at room temperature for 4 h after which the PE film was removed from the solution containing the free (unbound) particles, washed with EtOH, and then air-dried. Free and surface-bound nonmodified SiO_2 particles (nMSPs) were similarly prepared with the parameters previously described, with 1.5 mL of TEOS added to the solution in the absence of MPTES.

2.2.2. Antifog Coating on Organically Modified SiO_2-Coated PE Film. Solutions containing 5 mL of EtOH, 500 mg of PEGDA, and varying concentrations of the photoinitiator irgacure 2959 (Figure 3) were prepared (Table 1). The

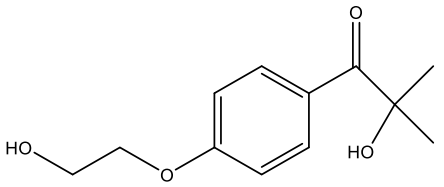

Figure 3. Chemical structure of irgacure 2959.

Table 1. Component Concentrations of the Antifog Coating Solution

sample	EtOH (mL)	PEGDA (gr)	irgacure 2959% (w/v)
1	5	0.5	0.02
2	5	0.5	0.05
3	5	0.5	0.1
4	5	0.5	0.5
PE/P(PEGDA)	5	0.5	0.05

solution was then spread on the OMS or nMSP-coated PE films with a size 1 Mayer rod with a wet deposit thickness of 6 μm (RK Print Coat Instruments Ltd., Litlington, Royston). The coated films were then cured under a 365 nm UV lamp until the coated film was dried.

An additional sample (PE/P(PEGDA)) was coated using the same parameters of sample 2 without a prior coating of OMS particles.

2.3. Characterizations. *2.3.1. Dynamic Light Scattering (DLS).* The hydrodynamic diameter and diameter distribution of the free particles in an aqueous continuous phase were determined by dynamic light scattering (DLS) with photon cross-correlation spectroscopy (Nanophox particle analyzer, Sympatec GmbH, Germany).

2.3.2. High-Resolution Scanning Electron Microscope (HRSEM). For dry size and size distribution imaging and morphological characterization of the free and surface-bound SiO_2 particles, high-resolution scanning electron microscope (HRSEM) images were taken using an FEI XHR-SEM Magellan 400 L scanning electron microscope operating at 5 kV. A drop of dilute aqueous samples containing the free SiO_2 particles was spread on a silicon wafer and dried at room temperature. The dried samples were coated with iridium in vacuum before viewing under HRSEM.

For characterization of the dry-coated polymer films, the films were attached to the silicon wafer with carbon tape, coated with iridium in vacuum, and then studied by HRSEM.

2.3.3. Atomic Force Microscope (AFM). AFM measurements were performed with a Bio FastScan scanning probe microscope (Bruker AXS). All images were obtained using the PeakForce QNM (PeakForce quantitative nanomechanical mapping) mode with a FastScan C (Bruker) silicon probe (spring constant of 0.45 N/m).

https://doi.org/10.1021/acsomega.1c07293
ACS Omega 2022, 7, 20505−20514

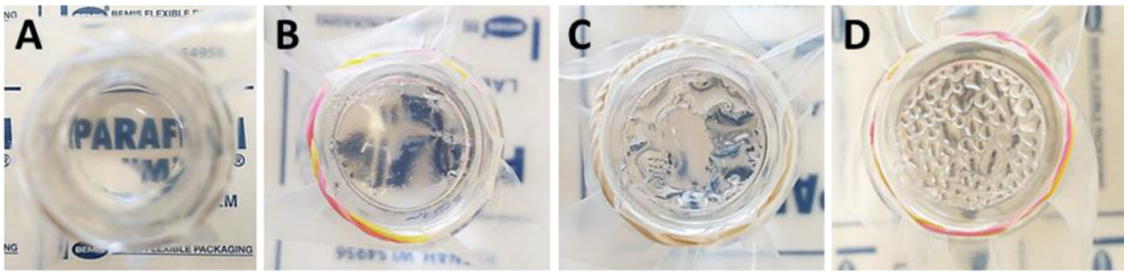

Figure 4. Illustration of different grades given to polymeric films after the hot-fog test. A thin, clear layer of water with no optical damage (A). Large, separate drops on the film surface resulting in lower transparency (B). Medium, separate drops on the film surface resulting in lower transparency (C). Small, separate drops on the film surface resulting in a foggy surface (D).

Table 2. Measured Hydrodynamic Diameters of Free nMSPs and OMS Particles and Dry Diameters of Both Free and Bound nMSPs and OMS Particles

	free particles	bound particles	
sample	hydrodynamic diameter (nm)	dry diameter (nm)	dry diameter (nm)
nMSP	214 ± 30	189 ± 8	126 ± 7
OMS	178 ± 25	163 ± 10	148 ± 29

The measurements were performed under environmental conditions in the acoustic hood to minimize vibrational noise. The images were captured in the retrace direction at a scan rate of 1.6 Hz. The image resolution was 512 samples/line. For image processing and thickness analysis, Nanoscope Analysis software was used. The "flattening" and "planefit" functions were applied to each image.

2.3.4. Attenuated Total Reflectance (ATR). ATR measurements of the coated and uncoated corona-treated PE films were done using a Bruker α-FTIR QuickSnap sampling module equipped with a platinum ATR diamond module.

2.3.5. Contact Angle (CA). Sessile drop water contact angle measurements were performed using a goniometer (System OCA, model OCA20, Data Physics Instruments Gmbh, Filderstadt, Germany). Double distilled water drops of 3 μL were placed on four different areas of each film and images were captured a few seconds after deposition. The static water contact angle values were determined by Laplace−Young curve fittings. All measurements were done under same conditions.

2.3.6. Ultraviolet−Visible Spectroscopy (UV−Vis). UV−vis spectra of the films in the range of 200−600 nm were determined in transmission mode using a Cary 5000 spectrophotometer (Agilent Technologies Inc.).

2.3.7. Hot-Fog Test. Antifogging properties were evaluated using the hot-fog test, which simulates real fogging conditions. A 20 mL vial was filled with 5 mL of water, after which the polymeric film sample was placed with the treated side facing the water and secured onto the vial opening. The vial was then heated at 60 °C for three hours resulting in water condensing onto the treated polymeric film sample. Visibility of the sample was periodically observed and was graded each time from A (completely transparent) to D (completely fogged) (Figure 4).

2.3.8. Durability Tests. Various durability tests were performed on the antifogging coating including immersion in different levels of pH, immersion in an aqueous surfactant solution, and tape test. These tests were done to examine the strength of the interaction between the coating and the film.

pH Immersion. HCl (32%) and NaOH were used to achieve the desired pH levels. Aqueous solutions of pH 1, 7, and 13 were prepared after which the coated film was immersed for 1 h. Subsequently, the coated film was washed with water, dried, and then exposed to a hot-fog test after each pH level immersion.

Surfactant immersion. A commercially available detergent was used as the surfactant in this test. The coated films were immersed in the aqueous surfactant solution for 1h. Subsequently, the coated film was washed with water, dried, and then exposed to a hot-fog test.

Tape test. The tape test consisted in firmly pressing an adhesive tape onto the coated film and then slowly peeling it off as described in the literature.[29] The tape was applied 10 times to the coated film after which the coated film was exposed to a hot-fog test. This procedure was performed several times as needed.

Sand test. Sand was placed on the surface of the coated film, which was removed by washing the contaminated surface with water. The film was then exposed to a hot-fog test.

3. RESULTS AND DISCUSSION

3.1. Free and Bound OMS Particles and nMSPs. Free and surface-bound OMS particles and nMSPs were prepared, as described in Section 2.2.1, by in situ polymerization of TEOS in the presence or absence of MPTES in an appropriate continuous phase containing EtOH and DDW under basic conditions. The presence of corona-treated PE films throughout the polymerization process resulted in surface-bound OMS particles (PE/OMS) and nMSPs (PE/nMSPs), which were grown on the surface of the corona-activated films.

3.2. Dynamic Light Scattering and High-Resolution Scanning Electron Microscope (HRSEM). DLS and HRSEM were used to measure the hydrodynamic and dry diameters of both free and bound OMS particles and nMSPs. Table 2 shows that the hydrodynamic diameters of the free nMSPs and OMS particles are larger than those of the dry particles, e.g., 214 ± 30 and 189 ± 8 nm, respectively, for the nMSPs and 178 ± 25 and 163 ± 10 nm, respectively, for the OMS particles. This difference is due to the water layer absorbed on the surface of the particles dispersed in the continuous phase as measured by the hydrodynamic measurements. Table 2 also illustrates that bound OMS particles are larger than bound nMSPs (148 ± 29 and 126 ± 7 nm, respectively) but free OMS particles are smaller than free

https://doi.org/10.1021/acsomega.1c07293
ACS Omega 2022, 7, 20505−20514

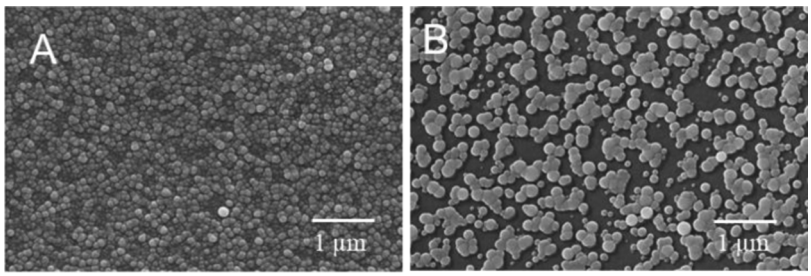

Figure 5. SEM images of PE films coated with nMSPs (A) and OMS particles (B).

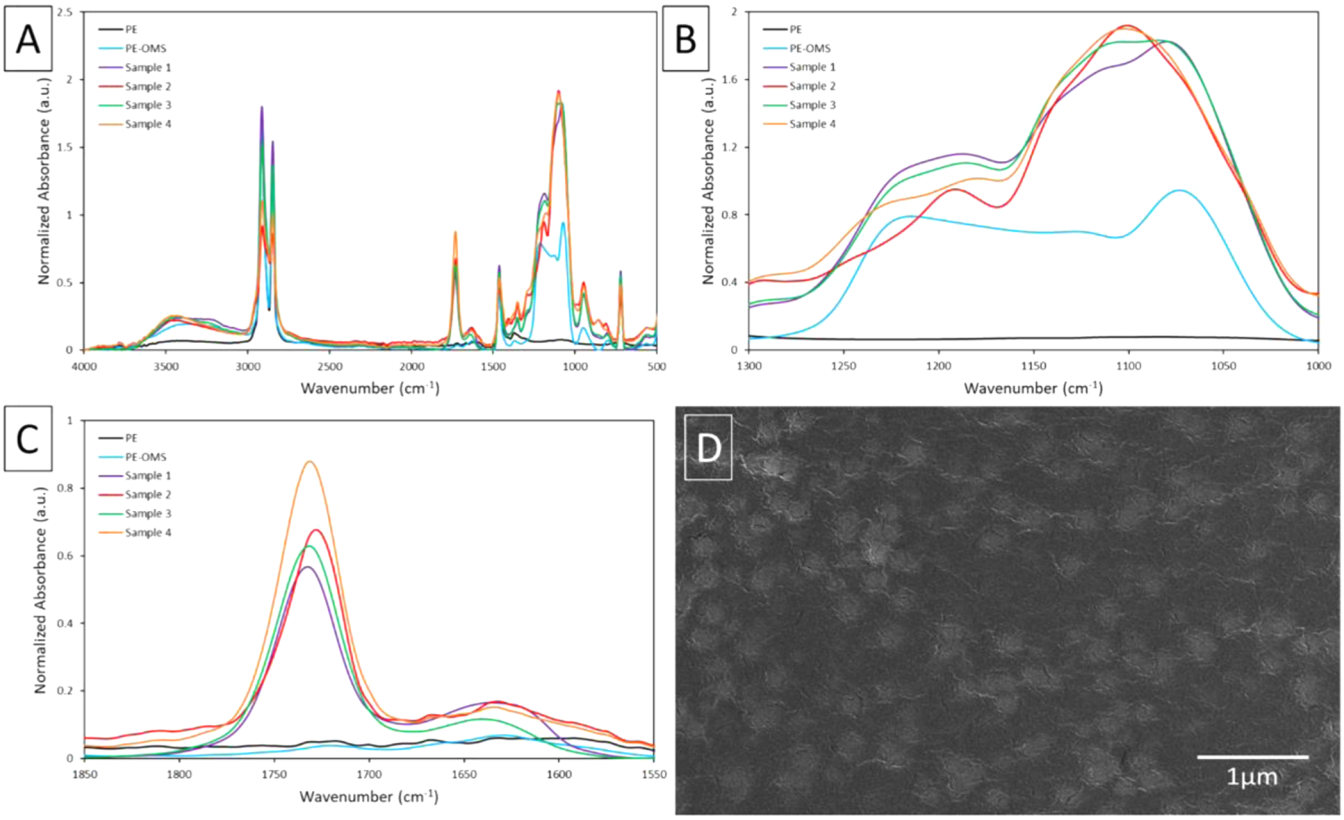

Figure 6. Full FTIR spectra of a corona-treated PE film (PE), a PE film coated with OMS particles (PE/OMS) and samples 1−4 (A). FTIR spectra in the range of 1000−1300 (B) and 1550−1850 (C). HRSEM image of sample 2 (D).

nMSPs (163 ± 10 and 189 ± 8 nm, respectively). The smaller free OMS particle size can be due to the steric hindrance from the carbon chain of MPTES, which would hinder the growth of the particles, resulting in more particle nucleation sites in the solution. Consequently, more OMS particles were formed but are smaller in size as compared to nMSPs.

The larger size of bound OMS particles can be explained by the SEM images taken of PE films coated with nMSPS and OMS particles (Figure 5). Figure 5B shows that the OMS-coated film is more sparsely coated than the nMSP-coated film (Figure 5A). The tightly packed nMSP coating restricts the growth of bound nMSPs beyond a certain size due to its close proximity to neighboring particles. Conversely, the OMS particle coated film, being more sparsely coated, has sufficient space to continue growing until all monomers are depleted from the solution allowing for larger bound particles.

3.3. UV Cured Polymerized PEGDA Coating. As previously stated, a combination of hydrophilic surface chemistry and smooth surfaces are properties typically desired to achieve antifog surfaces. To this aim, a solution of EtOH with PEGDA and irgacure 2959 was spread on the OMS- and nMSP-coated PE films to produce smooth and hydrophilic PE/OMS-P(PEGDA) and PE/nMSP-P(PEGDA) surfaces, respectively. Various concentrations of irgacure 2959 (0.02, 0.05, 0.1, and 0.5% w/v) were investigated due to the hydrophobic functional groups of irgacure 2959 (methyl and benzyl), which were thought to have a negative influence on the antifogging properties of the film. Additionally, changes in the photoinitiator concentration can influence the molecular weight of the resulting P(PEGDA) polymer coating, which can affect stability. The PEGDA-coated films were placed under a UV lamp, which initialized its radical polymerization to form a dry thin coating, anchoring the P(PEGDA) to the PE surface for a more stable coating. The average thickness of the P(PEGDA) coating was calculated to be 600 nm according to eq S1.

3.4. Attenuated Total Reflectance. Elemental compositions of the coated films were measured using ATR to

https://doi.org/10.1021/acsomega.1c07293
ACS Omega 2022, 7, 20505−20514

Table 3. Measured Water Contact Angles of PE, PE/nMSP, PE/OMS, PE/OMS-P(PEGDA) (samples 1−4), and PE/P(PEGDA) Films

				PE/OMS-P(PEGDA)				
sample	PE	PE/nMSP	PE/OMS	1	2	3	4	PE/P(PEGDA)
contact angle (°)	95 ± 1	38 ± 0.5	75 ± 2	<5	10 ± 1	44 ± 5	47 ± 2	13 ± 5

Table 4. Measured Surface Roughness of an Untreated PE Film (PE), a PE Film Coated with nMSPs (PE/nMSPS) and OMS Particles (PE/OMS), Samples 1−4, and a PE Film Coated with p(PEGDA)

				PE/OMS-P(PEGDA)				
sample	PE	PE/nMSP	PE/OMS	1	2	3	4	PE/P(PEGDA)
Rq (nm)	21 ± 7	20 ± 3	35 ± 9	2 ± 0.3	3 ± 0.4	16 ± 3	6 ± 2	21 ± 3

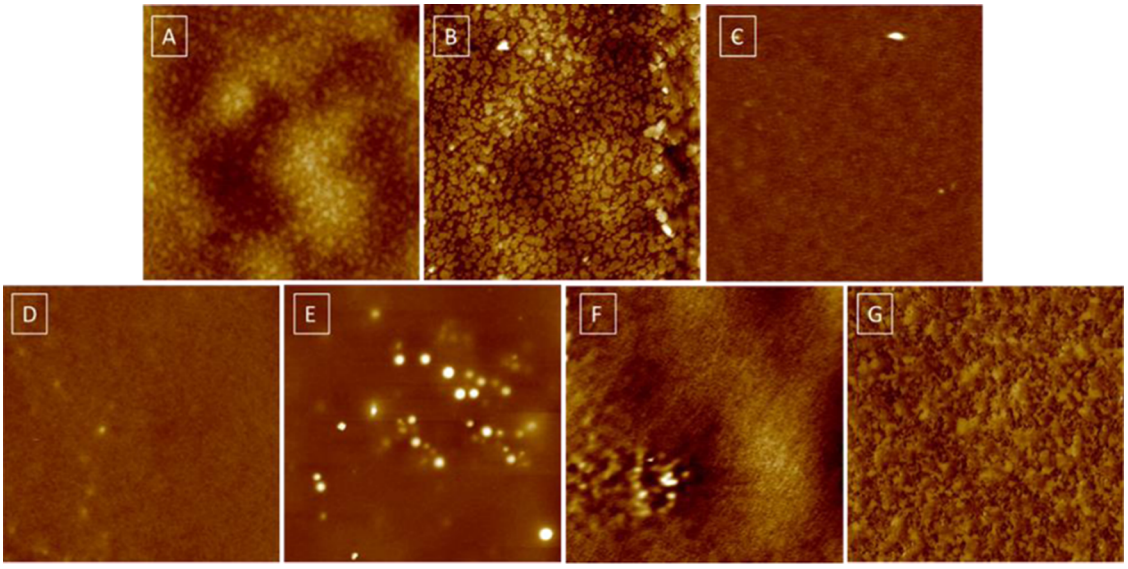

Figure 7. AFM images of corona-treated PE (A), PE-OMS (B), samples 1−4 (C−F, respectively), and PE/P(PEGDA) (G).

determine the presence of the OMS and P(PEGDA) coatings (Figure 6A). The characteristic peaks of PE at 719, 1468, 2851, and 2920 cm^{-1} are easily discernable in all spectra. The PE/OMS spectrum (blue line) shows that the Si−O−Si broad peak at the range between 1000−1300 cm^{-1} (Figure 6B) appears for the PE/OMS spectrum, which indicates the presence of surface-bound OMS particles. The peak at 1720 cm^{-1}, corresponding to the CO stretch of ester groups, indicates the presence of the PEGDA acrylate groups in the PE/OMS-P(PEGDA) sample (Figure 6C). The CO peak corresponding to the acrylate group of MPTES for the PE/OMS sample is not identified since MPTES constituted only 10% of the total monomer used while a larger amount of PEGDA was used for the antifog coating. Peaks for saturated ethers (C−O−C and C−O stretches) found on PEGDA are in the range between 1070 and 1140 cm^{-1}, which causes a slight deformation of the broad peak of Figure 6B for sample 1−4. An HRSEM image of a PE/OMS-P(PEGDA)-coated film was taken (Figure 6D). The bound OMS particles are visible in Figure 6D but appear hazy due to the additional P(PEGDA) coating.

3.5. Contact angle. Water sessile contact angles were measured to determine the changes in surface wetting as a result of the different coatings (Table 3). The PE/OMS and PE/nMSP coatings exhibit relatively high contact angles (75 ± 2 and 38 ± 0.5°, respectively). The higher contact angle of PE/OMS is due to the hydrophobic methacrylate groups of MPTES and the nonuniformity of the MPTES coating, which exposes the hydrophobic PE substrate (Figure 5B). The PE/P(PEGDA) sample exhibits a relatively low contact angle (13 ± 5°) due to the hydrophilic nature of PEG. Samples 1 and 2 of the PE/OMS-P(PEGDA) coating showed significantly lower contact angles (<5 and 10 ± 1°, respectively) than samples 3 and 4 (44 ± 5 and 47 ± 2°, respectively). This can result from the higher concentration of irgacure 2959 for both samples. The hydrophobic methyl and benzyl groups present on irgacure 2959 increase the hydrophobicity of the coated film surface so that high enough concentrations of irgacure 2959 can have an effect on surface properties. The surface roughness of the samples is not significantly different as shown in Table 3. This suggests that the surface roughness has little impact on their contact angle measurements. The 3 μL volume of the drop used to measure contact angles can easily overcome the slightly roughened surface structures to spread across the hydrophilic P(PEGDA) surface.

3.6. Atomic Force Spectroscopy (AFM). As stated previously, a low surface roughness is typically preferable for antifogging surfaces. Surface roughness of the samples was measured using AFM (Table 4 and Figure 7). As expected, the OMS particle coating (Figure 7B) increased the surface roughness due to the nonuniformity of the coating (Figure 5B). Relative to the OMS coating, the surface roughness of samples 1−4 significantly decreased as a result of the P(PEGDA) coating (Figure 7C−F). Conversely, PE/P-

https://doi.org/10.1021/acsomega.1c07293
ACS Omega 2022, 7, 20505−20514

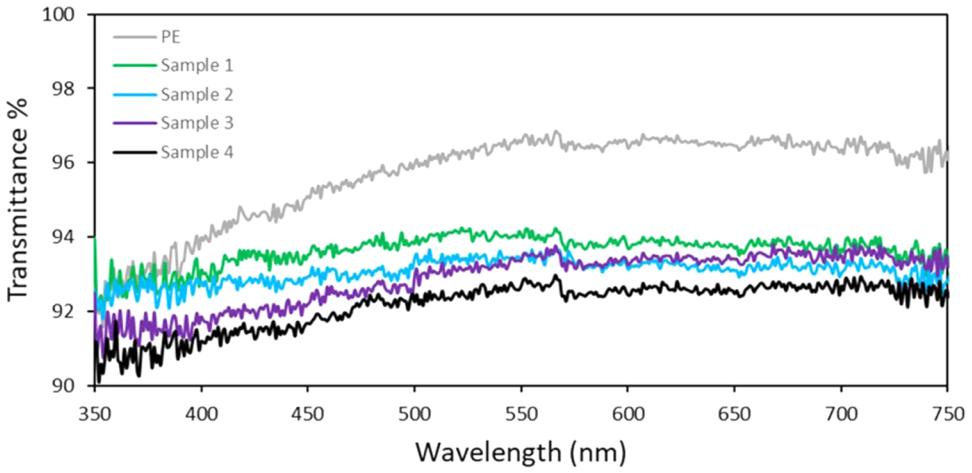

Figure 8. Transmittance UV−vis measurements of all OMS-coated samples and an uncoated PE film.

Table 5. Antifog Grades (A−D) Given to PE/OMS-P(PEGDA)-Coated Samples 1−4 Compared to PE Samples Coated with OMS, nMSPs, or P(PEGDA) over a 180 min Period[a]

		test time (min)						
sample		5	10	20	30	60	120	180
PE		D	D	D	D	D	D	D
PE/nMSP		C−D	D	D	D	D	B	A−B
PE/OMS		C−D	D	D	D	D	D	D
PE/OMS-P(PEGDA)	1	B	A−B	A	A	A	A	A
	2	A	A	A	A	A	A	A
	3	C	C	D	D	D	D	D
	4	C	D	D	D	D	D	D
PE/P(PEGDA)		C	D	D	D	D	C	A
AF spray		A	A	A	A	A	A	A

[a]The commercial AF spray was tested as well.

(PEGDA) exhibited the highest roughness of the PEGDA-coated samples (Figure 7G). This can be caused by the lack of good chemical compatibility between the hydrophilic p-(PEGDA) coating and the hydrophobic PE. These factors cause the PEGDA monomers dissolved in EtOH to amass and aggregate with one another so as to maximize surface tension. Conversely, the OMS layer of samples 1−4 increases the surface hydrophilicity due to additional hydroxyl groups that dominate the surface of the OMS particles, thus increasing chemical compatibility. Due to the AFM and contact angle results, it is clear that low concentrations of irgacure 2959 and the hydrophilicity of PEGDA had a greater influence on surface wetting than surface roughness.

3.7. Coating Transparency. Retaining film transparency after coating is an important factor that is required for use in antifogging applications. For this, all OMS-coated films were measured using UV−vis and compared to an uncoated film. Figure 8 shows that all samples, coated and uncoated, exhibited similar transparencies between 350 and 750 nm (90−96% transmittance). The similar transparency results between the coated and uncoated films are due to the thickness and smoothness of the coated P(PEGDA) layer. Thicker and rougher coatings increase light scattering, which results in a more opaque surface and vice versa.[30,31] Table 4 shows that samples 1−4 exhibit a low surface roughness (2−16 nm) while the average surface thickness was calculated to be 600 nm (eq S1). This means that the P(PEGDA) coatings of samples 1−4 will have a negligible effect on light scattering and will appear transparent.

3.8. Hot-Fog test. The hot-fog test was applied to all PEGDA-coated samples as described in Section 2.3.7. Table 5 shows the grades given to each sample using the grading system described in Figure 4. PE/nMSP, PE/OMS, and PE/P(PEGDA) exhibit poor antifog properties similar to the uncoated PE. These results are due to the absence of one or more surface criteria (hydrophilic chemical groups and a low surface roughness) needed for attaining antifog properties. The poor performances of control samples PE and PE/OMS are due to a lack of sufficient hydrophilic groups while both PE/nMSP and PE/P(PEGDA) exhibited a high surface roughness (Table 4). Despite their high surface roughness, PE/nMSP and PE/P(PEGDA) showed an improvement in their antifog properties at 120 and 180 min, respectively. This suggests that a hydrophilic surface can eventually achieve an antifogging effect on a relatively rough surface in a given enough time. The small fog droplets condense between the grooves of the rough surface, where they accumulate over time. Initially, the accumulated condensed droplets are trapped within the grooves, which gives the appearance of a fogged surface. The antifogging effect occurs only when the accumulation volume increases enough for the droplets to overcome their surrounding roughened surface. The effect of irgacure 2959 concentration on the antifog properties is made apparent, where higher concentrations of irgacure 2959 (0.1 and 0.5% w/v) exhibited poor visibility throughout the hot-fog test (C

https://doi.org/10.1021/acsomega.1c07293
ACS Omega 2022, 7, 20505−20514

Table 6. Antifog Stability Test of Sample 2, the PE/nMSP-P(PEGDA) Film, and AF Spray by Exposing Them to Multiple Hot-Fog Cycles

sample		cycle number[a]	test time (min) 5	10	20	30	60	120	180
PE/OMS-P(PEGDA)	2	1	A	A	A	A	A	A	A
		2	A	A	A	A	A	A	A
		3	A–B	A	A	A	A	A	A
		4	A	A	A	A	A	A	A
		10	A–B	A	A	A	A	A	A
PE/nMSP-P(PEGDA)		1	B	A–B	A–B	A–B	A–B	A–B	A
		2	C–D	C–D	D	D	D	D	D
AF spray		2	B	B	A–B	A–B	A	A	A
		3	B–C	B	B	B	B	A–B	A–B

[a]Each cycle consisted of a hot-fog test of 180 min, cooling overnight, and then an additional hot-fog test the day after.

and D), while lower concentrations (0.02 and 0.05% w/v) exhibited excellent visibility (A and A–B). This behavior could be explained by the hydrophobic nature of irgacure 2959, which, in higher concentrations, can cause the surface to become sufficiently hydrophobic, thus damaging the antifogging effect. The commercial AF spray was applied to a PE film and was also exposed to the hot-fog test and exhibited excellent antifogging properties as well.

3.9. OMS-P(PEGDA) Coating Stability and Durability.

Coating stability and durability are important factors in determining the effectiveness for real-world use. Sample 2 was selected to perform stability and durability tests due to its excellent antifog properties. Stability tests included multiple hot-fog test cycles, which consisted of a hot-fog test for 180 min, after which the sample was removed from the hot plate and left at room temperature overnight. The samples were then exposed to an additional hot-fog test for 180 min. As shown in Table 6, sample 2 was exposed to 10 hot-fog test cycles and exhibited excellent antifog properties throughout. Additionally, a similar test was performed on a PE film coated with nMSPs and a second layer of PEGDA with the parameters of sample 2 (PE/nMSP-P(PEGDA)). For the first hot-fog test cycle, the sample showed good antifog properties but decreased when exposed to the second cycle. This is due to the lack of bonds between the p(PEGDA) and nMSP layers, which causes the P(PEGDA) layer to migrate from the film. Conversely, sample 2 is able to withstand and remain stable through multiple exposures to the hot-fog test due to the interlayer covalent bonds. The commercial AF spray initially exhibited excellent antifogging properties, which decreased after additional hot-fog test cycles. These results can be compared to that of the PE/nMSP-P(PEGDA) coating in that the AF spray coating adheres to the surface using physical bonds. These bonds are typically less stable than covalent bonds over long exposure times.

Sample 2 and the AF spray coating were further exposed to different durability tests, which included immersion for 1 h in pH 1, 7, and 13 and immersion for 1 h in a solution of surfactants dissolved in water, sand tests, and tape test applications. Each of these tests was used to examine the range of stability for the coating against different external disturbances. Hot-fog tests were performed on the sample after each durability test. Sample 2 retained its excellent antifogging properties (grade A) for 3h after immersion in all pH levels and immersion in a surfactant solution and sand tests (Table S1). Conversely, the antifogging properties of the AF spray coating decreased to grade D after exposure to pH levels of 1, 7, and 13 as well as after surfactant and sand tests (Table S2). The samples were further exposed to 10 tape test applications, which slightly lowered the antifogging properties to grade A–B for the first 10 min but returned to grade A at 20 min until the completion of the hot-fog test. This suggests that the application of the tape tests deformed the surface slightly, which increased the surface roughness. A higher surface roughness briefly damaged the antifogging effects by causing the droplets to accumulate within the grooves on the surface as explained in Section 3.8. The droplets overcame the surface roughness between 10–20 min as shown in Table S3. This test was performed an additional two times on the same sample (10 tape tests were applied each time), which resulted in similar hot-fog test results (Table S3). This suggests that a small amount of PEGDA monomers was not covalently polymerized, which caused a slight initial coating deformation. Conversely, the AF spray coating exhibited decreasing antifogging properties throughout the hot-fog tests after tape test applications (Table S4). Sample 2 was measured using UV–vis after all durability tests were exposed to hot-fog tests for 3 h with no significant change in transparency (Figure S1). These durability test results of the antifog coating exhibit the robustness of these coated PE films against various external disturbances compared to the commercial AF spray. This is attributed to the strong covalent bonds between all of its components of the *in situ* synthesis to the surface in contrast to the physical bond adhesion of the AF spray coating.

4. CONCLUSIONS

Antifogging coatings were prepared in a two-step process using a modified Stöber method and UV curing. First, TEOS and MPTES were polymerized *in situ*, resulting in an OMS-coated PE film. The film was found to be nonuniformly coated with particles measured at 148 ± 29 nm. Next, a mixture of PEGDA and different concentrations of photoinitiator, irgacure 2959, was used to coat the PE/OMS film, which underwent UV curing. The PE/OMS-p(PEGDA) films were measured for contact angle, surface roughness, antifogging properties, stability, durability, and transparency. The films coated with 0.02 and 0.05% w/v of irgacure 2959 (samples 1 and 2, respectively) presented with the lowest contact angle and surface roughness. Additionally, these films exhibited excellent antifogging properties after being exposed to one hot-fog test cycle. Coating stability was determined by exposing the coated film to additional hot-fog test cycles. This consisted of drying the film and then exposing it to the additional hot-fog test. Sample 2 was found to exhibit excellent antifogging properties

https://doi.org/10.1021/acsomega.1c07293
ACS Omega 2022, 7, 20505–20514

even after 10 cycles. Additionally, all films were measured for transparency and durability against different pH levels ranging from 1−13, detergent contamination, and tape tests, which are important factors for antifogging films. All samples resulted in transparency similar to that of an uncoated PE film in the range between 90−96% transparency. Sample 2 was exposed to all durability tests and exhibited no change to its antifogging effects after exposure to pH 1, 7, and 13 for 1 h. Additionally, tape tests were applied to the film, which resulted in slight initial decrease to the antifogging effects of the film. The antifogging effects improved to grade A after 20 min. Furthermore, a sand test was performed, which showed no significant changes to the antifogging effects of the coated film. This indicates the stability of the coating given by the covalent bonds between all of the coating components to the PE film surface. This coating was compared to a PE film coated with a commercially available antifogging spray. Initially, the commercial spray exhibited excellent antifogging properties, which decreased substantially when exposed to the different durability tests. This *in situ* method offers a chemically simple, environmentally friendly, and relatively inexpensive process to achieve durable antifogging films with potential industrial uses.

■ ASSOCIATED CONTENT

Supporting Information

The Supporting Information is available free of charge at https://pubs.acs.org/doi/10.1021/acsomega.1c07293.

> Calculation of the dry coating thickness of coated samples; hot-fog test results for coatings using the *in situ* method and a commercial AF spray after durability tests of pH immersion, detergent immersion, and sand tests; hot-fog test results for coatings using the *in situ* method and a commercial AF spray after exposure to tape test applications; and UV−vis measurements immediately after durability test samples, which were exposed to a hot-fog test (PDF)

■ AUTHOR INFORMATION

Corresponding Author

Shlomo Margel − *Department of Chemistry, Institute of Nanotechnology and Advanced Materials, Bar-Ilan University, Ramat-Gan 5290002, Israel;* orcid.org/0000-0001-6524-8179; Phone: 972-3-5318861; Email: shlomo.margel@mail.biu.ac.il; Fax: 972-3-5318861

Author

Naftali Kanovsky − *Department of Chemistry, Institute of Nanotechnology and Advanced Materials, Bar-Ilan University, Ramat-Gan 5290002, Israel*

Complete contact information is available at: https://pubs.acs.org/10.1021/acsomega.1c07293

Notes

The authors declare no competing financial interest.

■ ACKNOWLEDGMENTS

The authors thank Dr. Michael Kanovsky for editing the manuscript and Dr. Eti Teblum for her assistance in AFM measurements.

■ REFERENCES

(1) Zhou, G.; He, J.; Xu, L. Antifogging Antireflective Coatings on Fresnel Lenses by Integrating Solid and Mesoporous Silica Nanoparticles. *Microporous Mesoporous Mater.* **2013**, *176*, 41−47.

(2) Zhang, L.; Li, Y.; Sun, J.; Shen, J. Mechanically Stable Antireflection and Antifogging Coatings Fabricated by the Layer-by-Layer Deposition Process and Postcalcination. *Langmuir* **2008**, *24*, 10851−10857.

(3) Introzzi, L.; Fuentes-Alventosa, J. M.; Cozzolino, C. A.; Trabattoni, S.; Tavazzi, S.; Bianchi, C. L.; Schiraldi, A.; Piergiovanni, L.; Farris, S. "Wetting Enhancer" Pullulan Coating for Antifog Packaging Applications. *ACS Appl. Mater. Interfaces* **2012**, *4*, 3692−3700.

(4) Wei, L.-J.; Yang, F.-X.; Du, Y.-P.; Chen, J.-Y.; Wang, H.-L. Fabrication and Characterization of Polyglycerol Fatty Acid Esters/Polyethylene Antifogging Film. *J. Food Process Eng.* **2017**, *40*, No. e12420.

(5) Ren, S.; Wang, L.; Yu, H.; Haroon, M.; Ullah, R. S.; Haq, F.; Khan, R. U.; Fahad, S. Recent Progress in Synthesis of Antifogging Agents and Their Application to Agricultural Films: A Review. *J. Coat. Technol. Res.* **2018**, *15*, 445−455.

(6) Mansoor, B.; Iqbal, O.; Habumugisha, J. C.; Xia, Z.; Jiang, R.; Chen, W. Polyvinyl Alcohol (PVA) Based Super-Hydrophilic Anti-Fogging Layer Assisted by Plasma Spraying for Low Density Polyethylene (LDPE) Greenhouse Films. *Prog. Org. Coat.* **2021**, *159*, No. 106412.

(7) Yoon, J.; Ryu, M.; Kim, H.; Ahn, G.-N.; Yim, S.-J.; Kim, D.-P.; Lee, H. Wet-Style Superhydrophobic Antifogging Coatings for Optical Sensors. *Adv. Mater.* **2020**, *32*, No. 2002710.

(8) Sun, Z.; Liao, T.; Liu, K.; Jiang, L.; Kim, J. H.; Dou, S. X. Fly-Eye Inspired Superhydrophobic Anti-Fogging Inorganic Nanostructures. *Small* **2014**, *10*, 3001−3006.

(9) Choi, M.; Xiangde, L.; Park, J.; Choi, D.; Heo, J.; Chang, M.; Lee, C.; Hong, J. Superhydrophilic Coatings with Intricate Nanostructure Based on Biotic Materials for Antifogging and Antibiofouling Applications. *Chem. Eng. J.* **2017**, *309*, 463−470.

(10) Cebeci, F. Ç.; Wu, Z.; Zhai, L.; Cohen, R. E.; Rubner, M. F. Nanoporosity-Driven Superhydrophilicity: A Means to Create Multifunctional Antifogging Coatings. *Langmuir* **2006**, *22*, 2856−2862.

(11) Wang, D.; Sun, Q.; Hokkanen, M. J.; Zhang, C.; Lin, F.-Y.; Liu, Q.; Zhu, S.-P.; Zhou, T.; Chang, Q.; He, B.; Zhou, Q.; Chen, L.; Wang, Z.; Ras, R. H. A.; Deng, X. Design of Robust Superhydrophobic Surfaces. *Nature* **2020**, *582*, 55−59.

(12) Zhi, J.; Zhang, L.-Z. Durable Superhydrophobic Surfaces Made by Intensely Connecting a Bipolar Top Layer to the Substrate with a Middle Connecting Layer. *Sci. Rep.* **2017**, *7*, No. 9946.

(13) Erbil, H. Y.; Demirel, A. L.; Avcı, Y.; Mert, O. Transformation of a Simple Plastic into a Superhydrophobic Surface. *Science* **2003**, *299*, 1377−1380.

(14) Choi, K.; Park, S. H.; Song, Y. M.; Lee, Y. T.; Hwangbo, C. K.; Yang, H.; Lee, H. S. Nano-Tailoring the Surface Structure for the Monolithic High-Performance Antireflection Polymer Film. *Adv. Mater.* **2010**, *22*, 3713−3718.

(15) Li, Y.; Xia, B.; Jiang, B. Thermal-Induced Durable Superhydrophilicity of TiO2 Films with Ultra-Smooth Surfaces. *J. Sol-Gel Sci. Technol.* **2018**, *87*, 50−58.

(16) Xiong, Y.; Lai, M.; Li, J.; Yong, H.; Qian, H.; Xu, C.; Zhong, K.; Xiao, S. Facile Synthesis of Ultra-Smooth and Transparent TiO2 Thin Films with Superhydrophilicity. *Surf. Coat. Technol.* **2015**, *265*, 78−82.

(17) Yuan, Y.; Liu, R.; Wang, C.; Luo, J.; Liu, X. Synthesis of UV-Curable Acrylate Polymer Containing Sulfonic Groups for Anti-Fog Coatings. *Prog. Org. Coat.* **2014**, *77*, 785−789.

(18) Bretler, S.; Kanovsky, N.; Iline-Vul, T.; Cohen, S.; Margel, S. In-Situ Thin Coating of Silica Micro/Nano-Particles on Polymeric Films and Their Anti-Fogging Application. *Colloids Surf., A* **2020**, *607*, No. 125444.

(19) Sason, E.; Kolitz-Domb, M.; Chill, J. H.; Margel, S. Engineering of Durable Antifog Thin Coatings on Plastic Films by UV-Curing of Proteinoid Prepolymers with PEG-Diacrylate Monomers. *ACS Omega* **2019**, *4*, 9352−9360.
(20) Chevallier, P.; Turgeon, S.; Sarra-Bournet, C.; Turcotte, R.; Laroche, G. Characterization of Multilayer Anti-Fog Coatings. *ACS Appl. Mater. Interfaces* **2011**, *3*, 750−758.
(21) Zheng, Z.; Liu, Y.; Wang, L.; Yu, L.; Cen, Y.; Zhu, T.; Yu, D.; Chen, C. A Novel Organic-Inorganic Zwitterionic Acrylate Polymer for High-Performance Anti-Fog Coating. *Prog. Org. Coat.* **2020**, *142*, No. 105578.
(22) Stöber, W.; Fink, A.; Bohn, E. Controlled Growth of Monodisperse Silica Spheres in the Micron Size Range. *J. Colloid Interface Sci.* **1968**, *26*, 62−69.
(23) Zhao, J.; Ma, L.; Millians, W.; Wu, T.; Ming, W. Dual-Functional Antifogging/Antimicrobial Polymer Coating. *ACS Appl. Mater. Interfaces* **2016**, *8*, 8737−8742.
(24) Sason, E.; Kolitz-Domb, M.; Cohen, S.; Grinberg, S.; Margel, S. Engineering of New Proteinoids and Proteinoid Nanoparticles of Narrow Size Distribution for Anti-Fog Applications. *J. Nanomedicine Nanotechnol.* **2017**, *8*, No. 1000473.
(25) Chang, C.-C.; Huang, F.-H.; Chang, H.-H.; Don, T.-M.; Chen, C.-C.; Cheng, L.-P. Preparation of Water-Resistant Antifog Hard Coatings on Plastic Substrate. *Langmuir* **2012**, *28*, 17193−17201.
(26) Howarter, J. A.; Youngblood, J. P. Self-Cleaning and Next Generation Anti-Fog Surfaces and Coatings. *Macromol. Rapid Commun.* **2008**, *29*, 455−466.
(27) Nuraje, N.; Asmatulu, R.; Cohen, R. E.; Rubner, M. F. Durable Antifog Films from Layer-by-Layer Molecularly Blended Hydrophilic Polysaccharides. *Langmuir* **2011**, *27*, 782−791.
(28) Syafiq, A.; Vengadaesvaran, B.; Pandey, A. K.; Rahim, N. A. Superhydrophilic Smart Coating for Self-Cleaning Application on Glass Substrate. *J. Nanomater.* **2018**, *2018*, No. e6412601.
(29) Rickerby, D. S. A Review of the Methods for the Measurement of Coating-Substrate Adhesion. *Surf. Coat. Technol.* **1988**, *36*, 541−557.
(30) Vorburger, T. V.; Marx, E.; Lettieri, T. R. Regimes of Surface Roughness Measurable with Light Scattering. *Appl. Opt.* **1993**, *32*, 3401−3408.
(31) Vargas, W. E.; Greenwood, P.; Otterstedt, J. E.; Niklasson, G. A. Light Scattering in Pigmented Coatings: Experiments and Theory. *Sol. Energy* **2000**, *68*, 553−561.

https://doi.org/10.1021/acsomega.1c07293
ACS Omega 2022, 7, 20505−20514